# Real-World Implementation of Adaptive Secondary Proportional Power Sharing in the Industry-Grade CMR Microgrid: A Case Study

Rakesh Shamrao Patekar, Mohanad Elsayed, Mohamed M. Zakaria Moustafa, Mahmoud Kabalan, Renuka Loka
*Center for Microgrid Research,University of St. Thomas,*
St. Paul, MN 55105
rakesh.patekar@stthomas.edu, elsa8648@stthomas.edu
mohamed.moustafa@stthomas.edu,
mahmoud.kabalan@stthomas.edu, loka3402@stthomas.edu

Thomas Bozada
*U.S. Army Engineer Research and Development Center,*
Champaign
IL

***Abstract*—Recent advancements in distributed energy resource (DER) technologies have accelerated the adoption of microgrids as resilient and flexible components of modern power systems. As the number of microgrids increases, the need for robust and validated secondary control strategies becomes essential to ensure reliable and stable operation. This paper presents the Real-world implementation of an adaptive secondary control scheme designed to achieve proportional power sharing among DER units according to their ratings in grid-connected mode. The proposed control strategy is first validated using a digital twin of the Center for Microgrid Research (CMR) microgrid developed on a Typhoon Hardware-in-the-Loop (HIL) platform. Subsequently, the controller is deployed and tested in the Real-world CMR microgrid. Experimental and simulation results consistently demonstrate the effectiveness and practicality of the proposed approach, exhibiting superior dynamic performance and stability compared to conventional PID-based secondary controller in real world applications.**

***Index Terms*—Adaptive PI control, Solar PV, BESS, Diesel Generators, Digital Twin, Micro-grid Secondary control, PCC power control.**

## I. Introduction

THE increasing use of distributed energy resources (DERs) and advances in converter technologies driving the adoption of diverse energy sources [1]. Microgrids integrate multiple DERs into a single system which can operate in both grid-connected and islanded modes and are controlled accordingly [2]. In grid-connected mode (GCM), surplus power can be fed back to the grid, while any power deficit can be supplied by the grid [3]. The microgrid controller plays a key role in managing active and reactive power in GCM without disrupting the system's stable operating points [4]. Many studies in the literature have proposed advanced methodologies to achieve proportional power sharing in GCM. However, most of these works remain limited to simulation or laboratory-scale validation, with few demonstrating Real-world implementation [5]. To ensure the robust functionality and reliability of microgrids, the proper design, field-validation and Real-world deployment of their control systems is essential [6].

Recent studies have proposed various optimization-based proportional–integral–derivative (PID) controllers using techniques such as Gray Wolf Optimization and neural network-based tuning, achieving improved stability and reduced overshoot in simulations [7], [8]. Advanced control strategies, including fractional-order PID, fractional PI, and cascaded PI/PID controllers have been reported in the literature for voltage and frequency restoration. However, their application for proportional power sharing remains limited [9]–[12]. Moreover, most of these approaches are restricted to simulations or laboratory setups, and their robustness against system variations and nonlinearities in Real-world microgrids has not been thoroughly validated. This underscores the need for practical implementation studies to ensure reliable and proportional power sharing.

This gap underscores the need for practical and field implementation of control strategies in Real-world microgrids that not only enhance dynamic performance—such as reducing transient overshoot, improving settling time, and increasing stability—but are also validated through Real-world testing. In this context, this paper presents the implementation of an adaptive PI-based secondary control strategy designed to achieve proportional power sharing according to DER ratings in GCM. In addition to Real-world implementation on an industry-grade microgrid, this study employs a digital twin model of the Center for Microgrid Research (CMR). The digital twin provides a hardware-accurate and realistic represen-

Effort sponsored by the U.S. Government under Other Transaction for Prototype Agreement number W9132T239C007 between UNIVERSITY OF ST. THOMAS and the Government. The U.S. Government is authorized to reproduce and distribute reprints for Governmental purposes notwithstanding any copyright notation thereon. The views and conclusions contained herein are those of the authors and should not be interpreted as necessarily repre senting the official policies or endorsements, either expressed or implied, of the U.S. Government.

This project was made possible in whole or in part by a grant from the Minnesota Department of Commerce through the Minnesota Renewable Development Account, which is financed by Xcel Energy ratepayers. Corresponding author: Mahamoud Kabalan Email: mahmoud.kabalan@stthomas.edu

979-8-3315-8138-1

tation of the microgrid's operational characteristics, enabling comprehensive analysis and validation of system performance. The key contributions of this paper are summarized as follows:

- Implementation of a adaptive PI-based secondary control for proportional power sharing in GCM, enabling precise active and reactive power regulation among Real-world microgrid resources while maintaining system stability.
- Validation of the adaptive PI control strategy using a digital twin model of the CMR microgrid on a real-time Typhoon Hardware-in-the-Loop (HIL) platform under various test scenarios.
- Implementation of an adaptive PI based proportional power sharing control technique using an off-the-shelf industrial Real-Time Automaton Controller (RTAC).

The remainder of this paper is organized as follows: Section II describes the CMR Microgrid system architecture and the integration of the secondary control with various DERs. Section III presents the implemented adaptive PI control methodology for proportional power sharing and compares its performance with a conventional PID controller. Section IV provides real-time simulation results obtained using the Typhoon HIL platform. Section V reports experimental results from the Real-world CMR Microgrid testbed. Finally, Section VI concludes the paper.

## II. The Real world CMR Microgrid - Test System

The real-time and experimental performance of the implemented adaptive PI-based secondary controller is verified and validated using the Real-world industry-grade CMR Microgrid. The CMR Microgrid consists of three DERs that supply power to the load, and it is capable of operating in GCM as well as ISM. The three primary sources in the system comprises a 62.5 kVA Diesel Generator (DiG),a 48 kW Solar Photovoltaic (PV), a 125 kW Battery Energy Storage System (BESS), and a 320 kVA load bank. The RTAC 3555 controller manages and controls various operations of the CMR microgrid for efficient and reliable performance. A schematic representation of the CMR microgrid is provided in Fig. 1, while the system parameters are detailed in Table I. The microgrid is connected to the utility grid through a 13.8kV/480V delta-to-wye transformer, with the microgrid operating at a voltage of 480 V. Control strategies depend on operation mode: in GCM, all sources use grid-following control; in ISM, DiG and BESS use droop control, while Solar PV is always in grid connected mode.

The primary control of different resources is not addressed in this literature, as the paper focuses on the secondary controller. Fig. 2 illustrates the schematic of the proposed secondary control architecture, highlighting the interaction between the secondary and primary control layers for the DiG, PV system, and BESS. Specifically, Fig. 2(a) depicts the control structure for the DiG. In GCM, it regulates the system by providing active power ($\Delta P$) and reactive power ($\Delta Q$) reference signals. Fig. 2(b) shows the control coordination for the BESS. Fig. 2(c) presents the P and Q reference for controlling the Solar PV system.

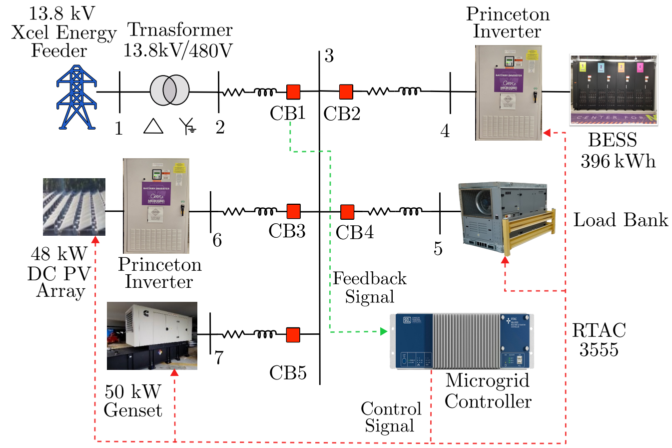


Fig. 1. Schematic of the CMR Microgrid with RTAC controller

TABLE I
System Parameters

| Sources | Value | Line Parameter | Value | |
|---|---|---|---|---|
| | | | R (pu) | X (pu) |
| DiG | 62.5 kVA | Line 7-3 | 0.15 | 0.03 |
| PV | 48 kW | Line 6-3 | 0.01 | 0.03 |
| BESS | 125 kVA | Line 4-3 | 0.01 | 0.04 |
| Load Bank | 320 kVA | Line 5-3 | 0.01 | 0.02 |
| System Voltage | 480 V | Line 2-3 | 0.01 | 0.01 |
| Utility Transformer | 300 kVA | $T_{UTIL}$ 1-2 | 0 | 0.06 |

## III. Methodology & Implementation

This section discusses the methodology and mathematical formulation of the adaptive PI control strategy, along with its implementation on both the Real-world and digital twin real-time microgrid model.

### A. Adaptive PI Based Secondary Control

In GCM, adaptive Pi based secondary controller ensures effective regulation of active and reactive power. Unlike conventional fixed-gain PID controllers, the adaptive PI controller autonomously adjusts its proportional ($K_p$) and integral ($K_i$) gains in response to system disturbances, thereby significantly improving transient stability and control accuracy. By modulating the gains based on the error magnitude, the controller achieves faster convergence and enhanced regulation performance. The mathematical formulation of the adaptive PI controller is developed in accordance with [10]–[12]. The equation for adaptive proportional gain($K_p$) is

$$K_p(t) = e^2(t) + K_1 \int e^2(t)dt \quad (1)$$

The term $e$ represents the error signal between the measured quantity and its corresponding reference value. The constant $K_1$ acts as the base gain for the ($K_p$). As the error signal $e$ varies, the overall proportional gain $K_p$ becomes adaptive, allowing dynamic tuning in response to system changes. Similarly, the adaptive integral gain ($K_i$) can be expressed using a formulation.

979-8-3315-8138-1

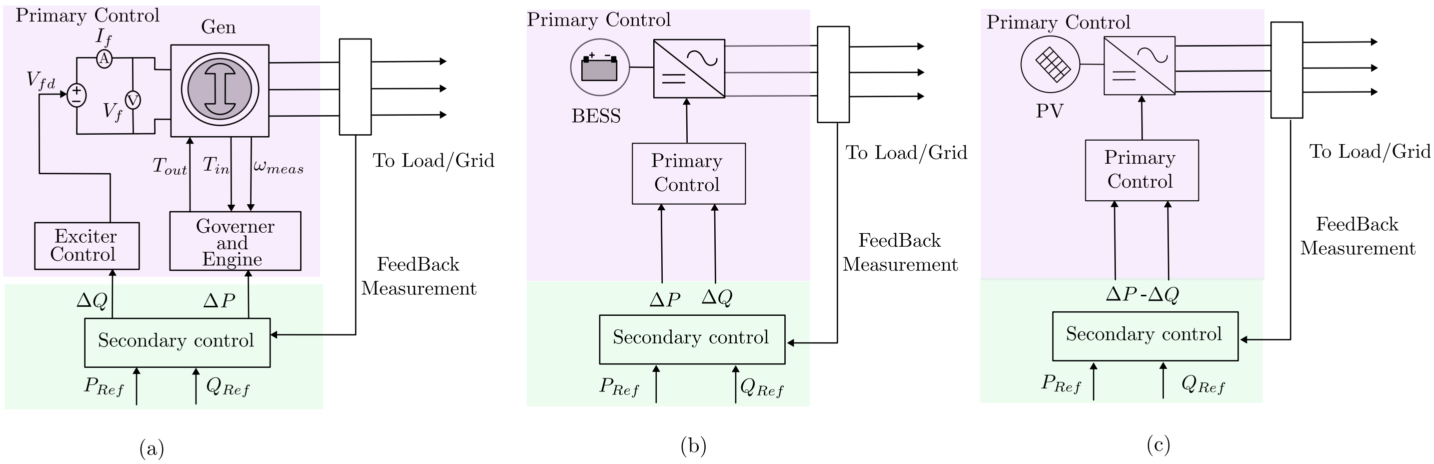


Fig. 2. Schematic representation of control interactions: (a) DiG control layers, (b) BESS control layers, (c) Solar PV control layers.

$$K_i(t) = K_2 \int e_i^2(t)dt \tag{2}$$

$K_2$ is the base gain for ($K_i$). By combining equations (1) and (2), the general form of the adaptive PI controller is obtained, as represented in (3). In this formulation, $K_3$ denotes the third base gain associated with the adaptive PI controller.

$$Output(t) = K_3 \left( K_p(t)e_i(t) + \int K_i(t)e_i(t)dt \right) \tag{3}$$

Equation (3), when transformed from the time domain to the Laplace (S) domain, can be equivalently expressed as (4).

$$Output(s) = K_3 \left( K_p(s)e + \frac{1}{s}K_i(s)e \right) \tag{4}$$

The coefficients $K_1$, $K_2$, and $K_3$ represent the adaptive gains of the controller. For the case of the CMR microgrid operating in GCM, the expressions for active and reactive power correction are given by (5) and (6) respectively. In this context, $\Delta P$ and $\Delta Q$ denote the correction terms for active power and reactive power, respectively.

$$\Delta P = K_3 \left( K_p e_p + \frac{1}{s}K_i e_p \right) \tag{5}$$

$$\Delta Q = K_3 \left( K_p e_Q + \frac{1}{s}K_i e_Q \right) \tag{6}$$

The active power error at the PCC, $e_P$, is defined as the difference between the reference and measured values and is expressed in (7), where $P_{Ref}$ denotes the reference active power and $P_{Meas}$ represents the measured active power at the PCC. Similarly, the reactive power error, $e_Q$, is the difference between the reference and measured reactive power, as shown in (8), where $Q_{Ref}$ is the reference reactive power and $Q_{Meas}$ is the measured reactive power at the PCC.

$$e_P = (P_{Ref} - P_{Meas}) \tag{7}$$

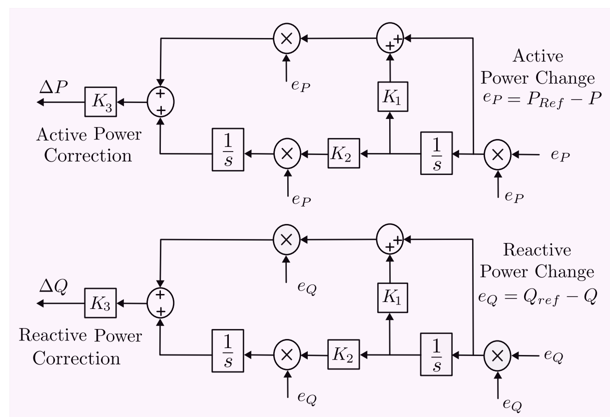


Fig. 3. Schematic representation of adaptive PI secondary control loops for proportional power sharing

$$e_Q = (Q_{Ref} - Q_{Meas}) \tag{8}$$

The block diagram shown in Fig. 3 provides a schematic overview of the proposed control strategy. Fig. 3 presents the corrective active power and reactive power reference assigned to each source to ensure proportional power sharing in GCM.

The gain tuning of the adaptive PI controller is a critical factor affecting its performance. It is a one-time process, and once optimized, the controller can maintain stable operation over a wide range of load variations. In this work, tuning is performed on the Typhoon HIL platform through multiple test runs to minimize steady-state error, overshoot, and settling time. The final gains for active power control at the PCC are $[K_1, K_2, K_3] = [1, 100, 1]$ and for reactive power control $[K_1, K_2, K_3] = [1, 500, 1]$.

### B. Comparison of Adaptive PI vs PID

A comparative analysis of the adaptive PI controller and a conventional PID controller is conducted using the same parameter set for GCM operation of the CMR Microgrid. The

979-8-3315-8138-1

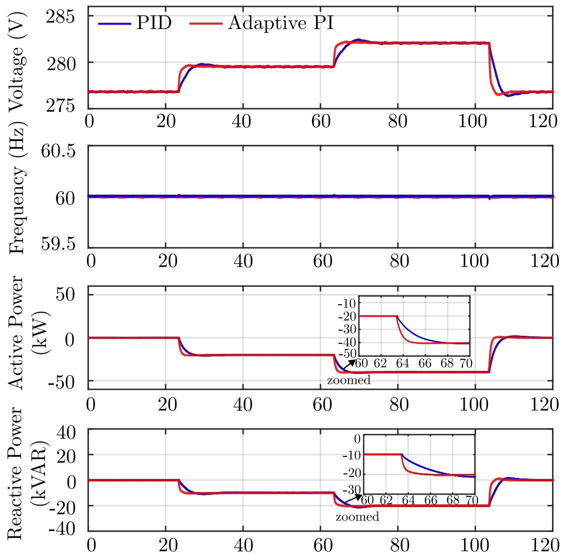


Fig. 4. Comparative analysis of adaptive PI with PID in GCM following PCC set points

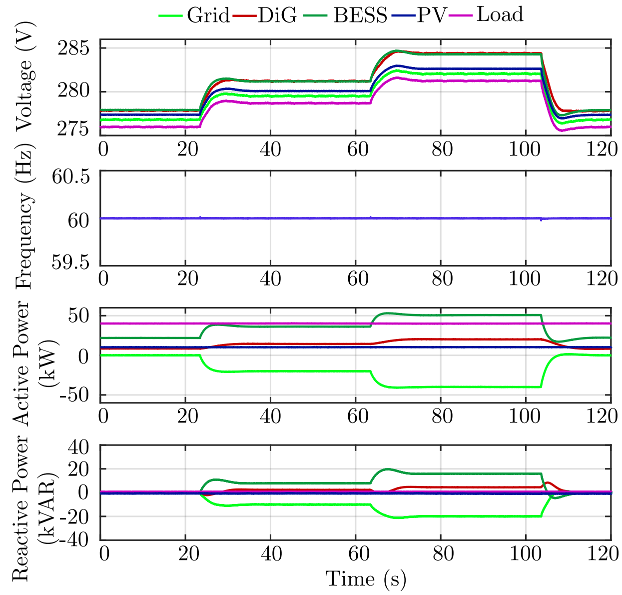


Fig. 5. GCM of the CMR Microgrid with adaptive PI secondary controller real-time simulation

output equation for conventional PID controller is represented as (9) [13].

$$G(s) = K_p + \frac{K_i}{s} + K_d s \tag{9}$$

Here, $K_p$, $K_i$, and $K_d$ denote the proportional, integral, and derivative coefficients, respectively, in the output function of the control system.

In GCM, as seen in Fig. 4 proportional power sharing is achieved with both controllers; however, the adaptive PI provides faster ( 4 sec compare to 7 sec by conventional PID) and more accurate corrective reference signals to the CMR sources, aligning them closely with the PCC set points for both active and reactive power.

## IV. Real Time Simulation Case study

As step before real world implementation this section presents the results of an adaptive PI-based secondary controller for proportional power sharing in GCM operation. The controller is implemented on a Digital Twin of the CMR Microgrid and tested in real time with single and multiple sources.

In Fig. 5 the PCC active and reactive power references ($P_{\text{set}}$ and $Q_{\text{set}}$) initially set to zero and sequentially stepped to 20 kW/10 kVAR, 40 kW/20 kVAR, and then back to zero. The grid power response (light green) closely follows the reference values, settling accurately at each set point. The negative power flow indicates that the grid absorbs power. A corresponding rise in PCC voltage is observed with changes in the reactive power reference, resulting from the reactive power support provided by the DERs. Fig. 5 further demonstrates that power sharing among the DERs is proportional to their ratings: the DiG supplies 30% and the BESS supplies 70% of both real and reactive power demands. The adaptive PI-based secondary controller achieves proportional power sharing without overshoot ensuring stable and smooth coordination among all DERs.

## V. The CMR Microgrid Case Study

This section presents the performance of the implemented adaptive PI-based secondary controller on a Real-world industry-grade microgrid system. Major implementation challenges included communication delays, PID saturation, and high transient responses, which complicated the direct application of simulated control strategies in practical scenarios. In addition, developing the adaptive structure in conjunction with the conventional RTAC PID framework presents further challenges. To address these issues, a realistic Controller HIL model was employed and thoroughly tested prior to Real-world deployment. The RTAC 3555 microgrid controller was utilized to implement the proposed adaptive PI-based secondary controller, ensuring seamless integration with the physical hardware. This configuration enables comprehensive validation of the controller's performance under actual microgrid operating conditions.

Fig. 6 and Fig. 7 present Real-world experimental results in GCM, showing proportional active and reactive power sharing in GCM. Fig. 6 shows the active power response of the DERs following changes in the PCC reference points. The reference was varied in steps from 0 kW to 10 kW, 20 kW, 30 kW, and then back to 20 kW, 10 kW, and finally 0 kW. The set power was proportionally shared between the BESS and DiG in a 70%–30% ratio, respectively.

Fig. 7 shows the reactive power response of the DERs following changes in the reactive power reference at the PCC. The reference was varied from 0 kVAR to 10 kVAR, and then to 20 kVAR, while keeping the active power fixed. In both cases, the DERs in the CMR microgrid accurately followed

979-8-3315-8138-1

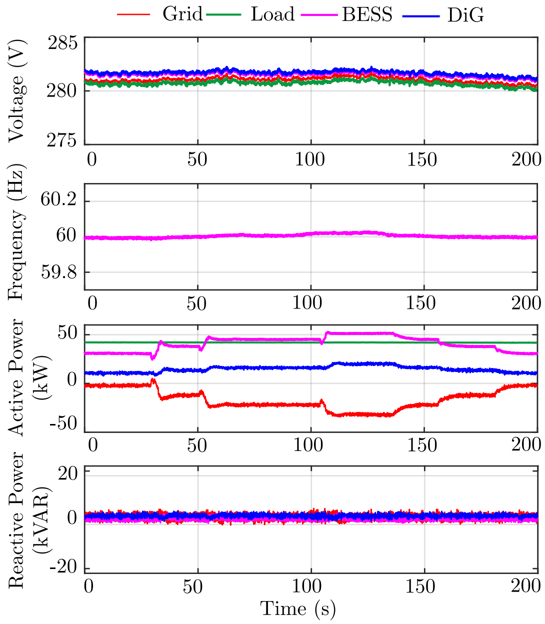


Fig. 6. Real world case study showing active power sharing in GCM with adaptive PI control

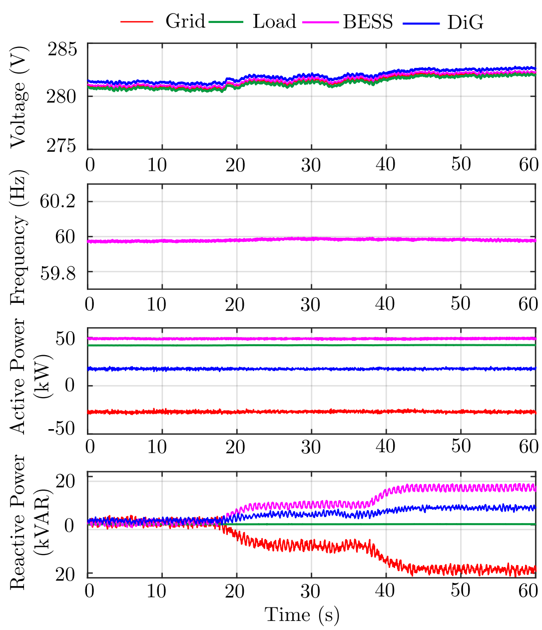


Fig. 7. Real world case study showing reactive power sharing in GCM with adaptive PI control

the setpoints without introducing oscillations, demonstrating the effectiveness of the proposed control algorithm in Real-world test scenarios.

## VI. Conclusion

This paper presented a Real-world implementation of an adaptive PI-based secondary control strategy for achieving proportional power sharing in a GCM. The proposed adaptive PI controller was validated through real-time simulations using a digital twin model of the CMR Microgrid. Simulation results demonstrated that the adaptive PI controller achieved faster settling times—up to twice as fast as the conventional PID controller—while exhibiting reduced overshoot and eliminating oscillations. The robustness of the control approach was further confirmed through multiple case studies involving various DER configurations and operating conditions.

Following successful real-time simulation validation, the controller was deployed on the Real-world industry-grade CMR Microgrid. Experimental results verified its practical effectiveness and suitability for Real-world deployment. Overall, the implemented adaptive PI-based secondary control provides a reliable, high-performance, and robust alternative to conventional PID controllers, demonstrating strong potential for widespread adoption in modern microgrid applications. Future work includes implementing an adaptive controller for both GCM and ISM modes of the microgrid.

## References


[1] Zhu, J., Yang, K., Lu, S., Sun, Q., Wu, Y. & Yuan, Y. An Objective-Oriented Aggregate Modeling Approach of Distributed Energy Resources. *IEEE Transactions On Smart Grid*. pp. 1-1 (2025)

[2] Han, Y., Zhang, K., Li, H., Coelho, E. & Guerrero, J. MAS-Based Distributed Coordinated Control and Optimization in Microgrid and Microgrid Clusters: A Comprehensive Overview. *IEEE Transactions On Power Electronics*. 33, 6488-6508 (2018)

[3] Olivares, D., Mehrizi-Sani, A., Etemadi, A., Cañizares, C., Iravani, R., Kazerani, M., Hajimiragha, A., Gomis-Bellmunt, O., Saeedifard, M., Palma-Behnke, R., Jiménez-Estévez, G. & Hatziargyriou, N. Trends in Microgrid Control. *IEEE Transactions On Smart Grid*. **5**, 1905-1919 (2014)

[4] Chen, K. & Baran, M. Robust Controller for Community Microgrids for Stability Improvement in Islanded Mode. *IEEE Transactions On Power Systems*. 38, 2472-2484 (2023)

[5] Gnana Swathika, O., Sarith Wasitha, M., Udayanga Hemapala, K. & Ramachandran, S. Design and Development of Research Level Microgrid Controller for Resilient and Sustainable Energy Management. *IEEE Access*. 13 pp. 59780-59789 (2025)

[6] Gu, H., Tamimi, B. & Cañizares, C. Improved Control and Stability Analysis of a Microgrid Connector Controller Under Unbalanced Network Conditions. *IEEE Transactions On Smart Grid*. 16, 2712-2724 (2025)

[7] Yakout, A., Dashtdar, M., AboRas, K., Ghadi, Y., Elzawawy, A., Yousef, A. & Kotb, H. Neural Network-Based Adaptive PID Controller Design for Over-Frequency Control in Microgrid Using Honey Badger Algorithm. *IEEE Access*. 12 pp. 27989-28005 (2024)

[8] Mishra, D., Nayak, P., Bhoi, S. & Prusty, R. Grey Wolf Optimization algorithm based Cascaded PID controller for Load-frequency control of OFF-Grid Electric Vehicle integrated Microgrid. *2020 IEEE International Symposium On Sustainable Energy, Signal Processing And Cyber Security (iSSSC)*. pp. 1-6 (2020)

[9] Ali, M., Kotb, H., Aboras, K. & Abbasy, N. Design of Cascaded PI-Fractional Order PID Controller for Improving the Frequency Response of Hybrid Microgrid System Using Gorilla Troops Optimizer. *IEEE Access*. 9 pp. 150715-150732 (2021)

[10] Sheida, K., Seyedi, M. & Ferdowsi, F. Adaptive Voltage and Frequency Regulation for Secondary Control via Reinforcement Learning for Islanded Microgrids. *2024 IEEE Texas Power And Energy Conference (TPEC)*. pp. 1-6 (2024)

[11] Dadi, R., K, M. & Damodaran, S. An adaptive PI based distributed control method to maintain accurate power sharing and voltage regulation in DC Microgrids. *2022 IEEE 19th India Council International Conference (INDICON)*. pp. 1-8 (2022)

[12] El-Ebiary, A., Mokhtar, M., Attia, M. & Marei, M. A Distributed Adaptive Control Strategy for Meshed DC Microgrids. *2023 IEEE Conference On Power Electronics And Renewable Energy (CPERE)*. pp. 1-6 (2023)

[13] Mohamed Ahmed Ebrahim Mohamed, Jagatheesan K. & Anand, B. Modern PID/FOPID controllers for frequency regulation of interconnected power system by considering different cost functions. *Sci Rep 13, 14084 (2023)*


979-8-3315-8138-1